

Universal Constants in Self-Organized Criticality Systems

MARKUS J. ASCHWANDEN¹

¹*Lockheed Martin, Solar and Astrophysics Laboratory (LMSAL), Advanced Technology Center (ATC), A021S, Bldg.252, 3251 Hanover St., Palo Alto, CA 94304, USA; e-mail: markus.josef.aschwanden@gmail.com*

ABSTRACT

The occurrence frequency distributions of fluxes (F) and fluences or energies (E) observed in the majority (in 18 out of 23 cases of astrophysical phenomena) are found to be consistent with the predictions of the fractal-diffusive self-organized criticality (FD-SOC) model, which predicts power law slopes with universal constants of $\alpha_F = (9/5) = 1.80$ for the flux, and $\alpha_E = (5/3) \approx 1.67$ for the fluence, respectively. The theoretical FD-SOC model is based on the fractal dimension, the flux-volume proportionality, and classical diffusion. The universal scaling laws predict the size distributions of numerous astrophysical phenomena, such as solar flares, stellar flares, coronal mass ejections (CME), auroras, blazars, active galactic nuclei (AGN), black-hole systems (BH), galactic fast radio bursts (FRB), gamma-ray bursts (GRB), and soft gamma-ray repeaters (SGB). In contrast we identify 5 outliers of astrophysical phenomena, including coherent solar radio bursts, random solar radio bursts, solar energetic particles (SEP), cosmic rays, and pulsar glitches, which are not consistent with the standard FD-SOC model, and thus require different physical mechanisms.

Keywords: methods: statistical — fractal dimension — self-organized criticality —

1. INTRODUCTION

Nonlinear physics operating in astrophysical systems that are governed by *self-organized criticality* (SOC) (Bak et al. 1987), has been studied in over 6000 publications, reaching out to almost every science discipline, such as planetary physics, solar physics, stellar physics, galactic physics, geophysics, biophysics, financial physics, or sociophysics, which have been described in the textbooks of Bak (1996), Jensen (1998), Ilachinski (2001), Hergarten (2002), Sornette (2004), Scott (2007), Aschwanden (2011a, 2013a, 2013b, 2019a, 2025), Pruessner (2012), Galam (2012), Charbonneau (2017). Most recent reviews have been presented in Watkins et al. (2016), Aschwanden et al. (2016); Sharma et al. (2016), and McAteer et al. (2016).

The concept of SOC has been evolved and expanded over time. Today we can distinguish between two schools: (i) the microscopic concept of cellular automaton algorithms (Bak et al. 1987), and (ii) the macroscopic concept of physical scaling laws (Aschwanden 2014, 2015, 2022). Instead of using the next-neighbor interactions of cellular automata, we quantify the spatial inhomogeneity in terms of the fractal dimension D_d for the Euclidean domains $d = 1$ (lines), $d = 2$ (areas), or $d = 3$ (volumes). Each fractal domain has a maximum fractal dimension of $D_d = d$, a minimum value of $D_d = d - 1$, and a mean value of $D_V = d - 1/2$ (Fig. 1),

$$D_V = \frac{(D_{V,\max} - D_{V,\min})}{2} = d - \frac{1}{2} . \quad (1)$$

For most applications in the (observed) 3-D world, the dimensional domain $d = 3$ is appropriate, which implies a fractal dimension $D_V = 2.5$. However, if 2-D areas are observed, the fractal dimension is $D_A = 1.5$ and the dimensionality is $d = 2$. In this work we will mostly make use of the 3-D fractal domain, while the 2-D domain is discussed elsewhere (e.g., Aschwanden 2022). The fractal volume V is then defined by the standard (Hausdorff) fractal dimension D_V in 3-D and the length scale L (Mandelbrot 1977),

$$V(L) \propto L^{D_V} . \quad (2)$$

We formulate the statistics of SOC avalanches in terms of size distributions (or occurrence frequency distributions) that obey the scale-free probability distribution function (Fig. 2), (Aschwanden 2014, 2015, 2022),

$$N(L)dL \propto L^{-d}dL , \quad (3)$$

where $d = 1, 2, 3$ represent the Euclidean dimensions of the fractal domains and L is the length scale of a SOC avalanche. From this scale-free relationship, the power law slopes α_x of other SOC parameters $x = [A, V, F, E, T]$ can be derived, such as for the area A , the volume V , the flux F , the fluence or energy E , and the duration T . The resulting power law slopes α_x can then be obtained mathematically by the method of variable substitution $x(L)$, by inserting the inverse function $L(x)$ and its derivative $|dL/dx|$,

$$N(x)dx = N[L(x)] \left| \frac{dL}{dx} \right| dL = x^{-\alpha_x} dx, \quad (4)$$

such as for the flux $x = F$,

$$\alpha_F = 1 + \frac{(d-1)}{D_V \gamma} = \frac{9}{5} = 1.80, \quad (5)$$

or for the fluence $x = E$,

$$\alpha_E = 1 + \frac{(d-1)}{d\gamma} = \frac{5}{3} = 1.67. \quad (6)$$

where γ is the nonlinearity coefficient in the flux-volume relationship,

$$F \propto V^\gamma = (L^{D_V})^\gamma, \quad (7)$$

which degenerates to proportionality $F \propto V$ for $\gamma = 1$. The proportionality between the (fractal) volume V and the (observed) flux V is depicted in Fig. (3). In astrophysical high-temperature plasmas, the volume V is approximately proportional to the number of electrons in a region of instability, while the flux F is proportional to the number of emitting photons, which implies that the photon-to-electron ratio is approximately constant and justifies the assumption of the flux-volume proportionality, in the case of incoherent emission mechanisms.

While this brief derivation of Eqs. (1)-(7) expresses the two main assumptions of fractality and linear flux-volume relationship for $\gamma = 1$, a third assumption needs to be brought in that takes the spatio-temporal evolution into account (e.g., see scale-free statistics of spatio-temporal auroral emission, Uritsky et al. 2002), which can be accomplished by the assumption of (classical) diffusive transport,

$$L \propto T^{\beta/2} = T^{1/2}, \quad (8)$$

with the transport coefficient $\beta = 1$. We call this model the *standard fractal-diffusive self-organized criticality (FD-SOC)* model, defined by $[d = 3, \gamma = 1, \beta = 1]$, while the generalized FD-SOC model allows for variable coefficients $[d, \gamma, \beta]$. Note that there is a subtle paradigm shift from microscopic to macroscopic concepts. The classical Bak-Tang-Wiesenfeld (1987) model mimics transport in SOC avalanches by cellular automaton redistribution rules in the microscopic world, while it is conceptualized by diffusive transport in models of SOC avalanches. We prefer the FD-SOC model in quantitative modeling of SOC processes, since cellular automaton algorithms require numerical methods and cannot be expressed analytically as a function of time. However, the diffusive transport in a SOC avalanche appears to generate similar avalanches as the next-neighbor interactions of cellular automata.

In this study we are testing the universality of power law slopes for fluxes ($\alpha_F = 1.80$) and fluences ($\alpha_E = 1.67$) for a set of 23 astrophysical phenomena. We find that most of the relevant observations are consistent with the standard FD-SOC model, but can identify also cases that require non-SOC models. In Section 2 we describe the data analysis and results, which include the selection of observations (Section 2.1), the definition of flux and fluence (Section 2.2), the nonparametric statistics of observed power law slopes (Section 2.3), the results of power law slopes for fluxes (Section 2.4) and fluences (Section 2.5), statistical outliers (Section 2.6), the nonlinear scaling of SEP events (Section 2.7), the effects of coherent and incoherent radiation (Section 2.8), the power laws of random size distributions (Section 2.9), and the establishment of universal constants in terms of the FD-SOC model (Section 2.10).

2. DATA ANALYSIS AND RESULTS

2.1. Selection of Observational Data

The input data used in this study covers a comprehensive data set of published occurrence frequency distributions (aka size distributions), obtained from publications that contain power law slopes of fluxes, (α_F), and fluences or energies, (α_E), observed and measured in astrophysical phenomena. The selection procedure involves searching and

identifying of relevant keywords in the titles and abstracts in publications, using the NASA Astronomical Database System (ADS). A list of 23 astrophysical phenomena is compiled in Tables 1 and 2, which span from solar distances to galactic scales. The third and fifth columns in Table 1 specify the means and standard deviations of published power law slopes, α_F and α_E , listed separately for fluxes and fluences of astrophysical phenomena. An estimate of the number of analyzed size distributions can be obtained from the sum of the cases, which amounts to ($\sum N_F = 170$) for fluxes, and ($\sum N_E = 104$) for fluences or energy, as listed in Table 1 (second and forth columns).

2.2. Definition of Flux and Fluence

The flux is defined in physical units of [energy/time], usually measured at the (background-corrected) peak flux F at the peak time t_p of an event,

$$F = \max[f(t = t_p)] - f_{BG} , \quad (9)$$

bound by the time range $t_1 \leq t_p \leq t_2$. The subtraction of an event-unrelated background flux f_{BG} is a particularly important correction for the smallest events of a size distribution, when they become comparable or smaller than the event-unrelated background flux.

The fluences have the physical unit of [energy], and are measured by the time integral of the time profile $f(t)$. Thus, the fluences (E) are the time-integrated fluxes,

$$E = \int_{t_1}^{t_2} [f(t) - f_{BG}] dt , \quad (10)$$

for a time interval (t_1, t_2) with well-defined start times t_1 and end times t_2 .

Details of the published power law slopes of size distributions (α_F , α_E) and references are given in Aschwanden et al. (2016); Aschwanden (2022, 2025), and Aschwanden and Gogus (2024), and are not repeated here for brevity reasons. Most of the processed information in this study is based on the means μ and standard deviations σ of the 23 astrophysical phenomena, for the SOC parameters F and E , as listed in Table 1.

2.3. Non-Parametric Statistics

We tabulate our findings of power law slopes of fluxes α_F and fluences α_E for each of the astrophysical phenomena in Table 1 and show their histograms in Fig. (4). The histograms in Fig. (4) contain astrophysical phenomena, which amounts to $N = 15$ values for the fluxes, and $N = 12$ for the fluences, respectively, where we excluded $N = 5$ non-SOC phenomena as described in the following.

From the two samples of phenomena in the histograms shown in Fig. (4) we calculate the means μ and standard deviations σ in the two histograms, which is a method of non-parametric statistics without any assumption on the functional shape of the size distributions $N(\alpha_F)$ and $N(\alpha_E)$. We find a distribution of $\alpha_F = 1.85 \pm 0.19$ for the fluxes, which is close to the theoretical FD-SOC prediction $\alpha_{f,theo} = 1.80$. Similarly, we find a distribution of $\alpha_E = 1.67 \pm 0.09$ for the fluences, which precisely matches the theoretical FD-SOC prediction $\alpha_{E,theo} = 1.67$. Note that the uncertainty of the power law slopes varies in the range of $\sigma/\mu \approx 5\% - 10\%$. Inspection of the deviation of power law slopes from ideal straight power laws reveal that most of the uncertainties occur for a variety of data analysis errors, such as neglected background subtraction, inadequate fitting range, small-number statistics, or may naturally manifest a non-SOC process.

2.4. Power Law Slopes of Fluxes

Let us investigate the results of the power law slopes α_F for fluxes, which are shown in form of histograms $N(\alpha_F)$ in Fig. 4 (top panel), while the dashed vertical line indicates the theoretically predicted value. We find the following 15 parameters with means μ and standard deviations σ : $\alpha_{\text{HXR}} = 1.74 \pm 0.11$ for solar flare hard X-rays, $\alpha_{\text{SXR}} = 1.87 \pm 0.10$ for solar flare soft X-rays, $\alpha_{\text{EUV}} = 1.68 \pm 0.16$ for solar EUV nanoflares, $\alpha_{\text{Inc}} = 1.80 \pm 0.21$ for solar incoherent radio bursts, $\alpha_{\text{CME}} = 2.01 \pm 0.35$ for coronal mass ejections, $\alpha_{\text{Aur}} = 1.79 \pm 0.21$ for magnetospheric aurora events, $\alpha_{\text{SF}} = 1.82 \pm 0.37$ for stellar flares, $\alpha_{\text{KEPLER}} = 1.87 \pm 0.29$ for stellar flares observed with KEPLER, $\alpha_{\text{TESS}} = 2.27 \pm 0.19$ for stellar flares observed with TESS, $\alpha_{\text{AGN}} = 1.73 \pm 0.19$ for active galactic nuclei events, $\alpha_{\text{BH}} = 1.65 \pm 0.25$ for black hole systems, $\alpha_{\text{BL}} = 1.98 \pm 0.08$ for blazars, $\alpha_{\text{GRB}} = 2.10 \pm 0.25$ for gamma-ray bursts, and $\alpha_{\text{SGR}} = 1.88 \pm 0.06$ for soft gamma-ray repeaters, $\alpha_{\text{XB}} = 1.52 \pm 0.45$ for X-ray binaries, which are mostly consistent with the predictions of the FD-SOC theoretical model within the statistical uncertainties, i.e., $\alpha_F = 1.80$. The variety of astrophysical source

locations, ranging from solar flares all the way to galactic events, underscores the universality of the FD-SOC model. The most discrepant case is coherent radio emission, ($\alpha_{\text{Coh}} = 1.29 \pm 0.12$), while incoherent radio emission displays excellent agreement ($\alpha_{\text{Inc}} = 1.80 \pm 0.21$) with the FD-SOC model ($\alpha_F = 1.80$). We will discuss below how coherent and incoherent radio emission indicate different plasma physics conditions.

2.5. Power Law Slopes of Fluences and Energies

The power law distributions for fluxes and fluences are not identical, and hence we expect different slope values, which are higher for fluxes, $\alpha_F = (9/5) = 1.80$, and are lower for fluences or energies, $\alpha_E = (5/3) \approx 1.67$. Therefore the FD-SOC model predicts this duality, which we are testing here. In Fig. 4, the thin vertical line indicates the observed mean power law slope μ , while the dashed vertical line depicts the theoretically predicted value. From various astrophysical observations we find the following 12 parameters (Table 2): $\alpha_{\text{HXR}} = 1.56 \pm 0.11$ for solar flare hard X-ray emission, $\alpha_{\text{SXR}} = 1.79 \pm 0.35$ for solar flare soft X-ray emission, $\alpha_{\text{CME}} = 1.84 \pm 0.41$ for coronal mass ejections, $\alpha_{\text{WIND}} = 1.70 \pm 0.17$ for solar wind fluctuations, $\alpha_{\text{Aur}} = 1.60 \pm 0.13$ for magnetospheric aurora events, $\alpha_{\text{TGF}} = 1.73 \pm 0.40$ for terrestrial gamma-ray flashes, $\alpha_{\text{BH}} = 1.73 \pm 0.25$ for black hole systems, $\alpha_{\text{BL}} = 1.63 \pm 0.17$ for blazars, $\alpha_{\text{FRB}} = 1.67 \pm 0.12$ for fast radio burst events, $\alpha_{\text{GRB}} = 1.68 \pm 0.24$ for gamma-ray bursts, $\alpha_{\text{SGR}} = 1.68 \pm 0.12$ for soft gamma-ray repeaters, $\alpha_{\text{XB}} = 1.53 \pm 0.04$ for X-ray binary events. The behavior of power law slopes is very similar for the flux α_F (Fig. 4, top panel) and fluence α_E (Fig. 4, bottom panel). Most of the observed mean values μ are consistent with the theoretical predictions of the FD-SOC model within the statistical uncertainties, except for 2 phenomena (SEP and cosmic rays) that are classified as non-SOC phenomena.

2.6. Statistical Outliers

The main hypothesis of this study is a statistical test whether the power law slopes of observed flux and fluence size distributions ($\alpha_x^{\text{obs}} \pm \sigma_x$) are consistent with the theoretical FD-SOC model (α^{theo}). We found that 18 astrophysical phenomena are consistent with the FD-SOC model within about one standard deviation (see Table 1), while 5 phenomena are found not to be consistent (Table 2), as discussed in the following.

The two phenomena of solar coherent radio bursts and solar energetic particles (SEP) show relatively flat power law slopes of $\alpha_F \approx \alpha_E \approx 1.3 \pm 0.1$ that cannot be reproduced by a FD-SOC model (with $\gamma = 1$), but can be produced by a generalized SOC model with a nonlinear flux-volume coefficient of $\gamma \approx 2$.

Cosmic rays have a relatively steep power law slope of $\alpha_E \approx 3.0 \pm 0.3$, which also cannot be produced with the FD-SOC model, but matches the predicted slope in a one-dimensional (1-D) Euclidean domain ($D_V = 1$).

Random solar radio bursts follow the random distribution of Poisson statistics by definition, which is contrary to the nonlinear power law statistics of SOC systems (with “fat tails” in their size distribution), and thus consequently cannot be reproduced by the FD-SOC model.

Finally, the fifth outlier, i.e., pulsar glitches, exhibit erratic size distributions that cannot be fitted with any power law distribution (see Cairns 2004; Melatos et al. 2008), which probably results from small-number statistics, background subtraction problems, inadequate fitting range, finite system-size effects, and other large deviations from ideal power laws.

In any case, what the 5 outliers have in common is their incompatibility with the FD-SOC model, which justifies their elimination from statistical tests, since they require different physical mechanisms. This is not a circular argument, because the FD-SOC model predicts unique parameters without free variables, such as the peak flux slope α_F or the fluence slope α_E of the investigated size distributions. We do not aim to derive the functional form of the statistical distribution $N(\alpha_x)$, but merely perform a test whether the observed power law slopes agree with the theoretically predicted values within the statistical uncertainties.

2.7. Solar Energetic Particle (SEP) Events

The anomaly of SEP events has been pointed out earlier and it was suggested that proton-emitting solar flares are a special class of events, requiring a different physical mechanism for the production of energetic protons (Cliver et al. 1991; Kahler 2013; Cliver and D’Huys 2018). In the derivation of the FD-SOC model we can distinguish two different processes in the flare evolution, $F \propto V^\gamma$, with $\gamma = 1$ for a slow linear evolution, and with $\gamma \approx 2$ for a fast nonlinear evolution, which is also a measure of the spatio-temporal evolution $F(t) \propto V(t)^\gamma$ of an individual flare event, in the statistical average. The nonlinearity coefficient γ is not predicted by the FD-SOC model, but can be estimated from the observations, by inverting the relationship $\alpha_F = 1 + (d - 1)/(D_V \gamma)$, which yields $\gamma = (d - 1)/(\alpha_F - 1)$.

Inserting a typical observational value of $\alpha_E \approx 1.4$, we obtain a coefficient of $\gamma = 2$, for the Euclidean space dimension $d = 3$. Thus, we can explain both the SEP events, $\alpha_F = 1.29 \pm 0.12$, as well as the solar coherent radio burst events, $\alpha_F = 1.36 \pm 0.26$, with the generalized SOC model, matching a nonlinear flux-volume coefficient of $\gamma \approx 2$.

2.8. Incoherent and Coherent Emission

Why does coherent radio emission, ($\alpha_{\text{Coh}} = 1.29 \pm 0.12$), has a different size distribution than incoherent radio emission ($\alpha_{\text{Inc}} = 1.80 \pm 0.21$)? In the Introduction we pointed out that the standard FD-SOC model is based on three fundamental assumptions (fractality, diffusive transport, and flux-volume proportionality), which defines a linear relationship between the observed flux and (fractal) volume, i.e., $F \propto V^\gamma$ with $\gamma = 1$ in the standard FD-SOC model. The resulting proportionality, $F \propto V$, implies then an equivalence between the corresponding power law slopes, i.e., $\alpha_F = \alpha_V$. This linear behavior is also called an incoherent or a random process. Incoherent emission processes occurring in the solar corona include, for example, thermal bremsstrahlung, gyroresonance emission, or gyro-synchrotron emission.

In contrast, a nonlinear behavior is typical for coherent emission, where the nonlinearity is expressed by the relationship $F \propto V^\gamma$, for $\gamma > 1$. Coherent emission entails exponential-growth processes during an instability, which is a typical nonlinear behavior. Such coherent emission processes occur when a particle distribution function becomes inverted by some dynamic process, such as by electron beam formation, or by loss-cone distribution functions, most conspicuously visible in electron-cyclotron microwave amplification by stimulated emission of radiation (MASER). The phenomenon of electron beams is driven by a positive gradient in the parallel velocity distribution function, while loss-cones are driven by perpendicular positive gradients in the velocity distribution function (see textbooks on plasma physics, e.g., Benz 1993, Sturrock 1994, Boyd and Sanderson 2003).

2.9. Random Size Distributions

There is another anomaly of substantial deviations from ideal power laws notable in at least 1 (out of the 23) cases, which we call *solar random radio bursts* and has been reported in 4 cases: a type I storm with $\alpha_F = 3.25 \pm 0.35$ (Mercier and Trotter 1997); a DCIM-S radio spike burst event with $\alpha_F = 2.99 \pm 0.63$; (Aschwanden et al. 1998); a microwave spikes event with $\alpha_F = 7.40 \pm 0.40$ (Ning et al. 2007); and a type I storm with $\alpha_F = 4.80 \pm 0.10$ (Iwai et al. 2013). This type of radio bursts clearly is not consistent with neither the standard FD-SOC model ($\gamma = 1$) nor with the generalized FD-SOC model ($\gamma > 1$). First of all, the 4 observations reported here are outside the theoretical physical range of SOC parameters, which is $1.0 \leq \alpha_x \leq 3.0$. Secondly, the power law fitting ranges are found to extend over very small ranges (often less than a decade), so that no reliable power law slope can be fitted. The most likely explanation for the too steep power law slopes is the confusion between the power law inertial range and the exponentially fall-off at the upper end of the size distribution. This transition from a power law to an exponential drop-off is dictated by the finite-system size limit of the largest events, which is expected to form a gradual roll-over within the range of $3.0 \lesssim \alpha_x < \infty$.

Most generally, the observed power law distribution functions can be fitted with a three-part model that includes (i) the flattening due to incomplete sampling of small events, (ii) the initial range that can be fitted with a pure power law function, and (iii) the steepening due to finite-system size effects for the largest events, approximated with an exponential function, following Poisson statistics. Such a generalized three-part size distribution function can be described by (Aschwanden 2021),

$$N(x)dx = N_0(x_0 + x)^{-\alpha_x} \exp\left(-\frac{x}{x_e}\right) dx, \quad (11)$$

Such a three-part size distribution may recover the convolved power law slope α_x , but it may blur the distinction between the FD-SOC model and a non-SOC model. The FD-SOC model requires a pure power law function, while the non-SOC model presented here requires a convolution of a power law with an exponential function. The inclusion of the exponential fall-off fits the Poisson statistics of random processes.

2.10. Universal Constants

It is often said that power laws are the hallmarks of SOC. Consequently, since power laws are measured by their slopes α_x , we can also say that the (slopes of) size distributions are the hallmarks of SOC. A variety of slope values α_x have been reported within a range of $1.5 \leq \alpha_x \leq 2.3$. The question arises now whether these constants α_x are universally valid and predictable, or are they individual for every astrophysical phenomenon and for every physical

process, and then are likely to be unpredictable. Our FD-SOC model suggests that every SOC parameter x has a predictable power law slope α_x that is universally valid, where the SOC parameters include the length scale L , the area A , the volume V , the flux F , the fluence or energy E , and the duration T . The predicted power law slope values are $\alpha_L = 3$, $\alpha_A = 7/3$, $\alpha_V = 9/5$, $\alpha_F = 9/5$, $\alpha_E = 5/3$, and $\alpha_T = 2$.

Why are these SOC parameters universally valid? The fundamental reason is that the underlying three assumptions are universal too, namely the fractality, the diffusive transport, and the flux-volume proportionality. The latter assumption implies a constant emissivity, i.e., flux density F per volume element V , i.e., $\varepsilon = F/V$. This assumption is an approximation only of course, but works satisfactorily for a variety of incoherent emission mechanisms in terms of the electron flux density or photon flux density (luminosity). Hence, the universality of the power law slopes α_x is a natural consequence of the universal existence of the scaling laws for the fractal dimension, $D_V = d - 1/2$, the diffusive transport, $L \propto T^{1/2}$, and the flux-volume linearity, $F \propto V$, for a FD-SOC model with Euclidean dimensionality $d = 3$.

3. SUMMARY AND CONCLUSIONS

Let us summarize our data analysis and conclusions:

1. We extracted a total of $\sum N_F = 170$ flux and $\sum N_E = 104$ fluence size distributions from the published literature, which are characterized by the power law slopes α_F and α_E . We group these 274 cases into 23 astrophysical phenomena, ranging from solar, stellar, terrestrial, magnetospheric to galactic distances. Histograms of the power law slopes are constructed for the fluxes and fluences separately. Astrophysical phenomena with large deviations from ideal power laws are likely to be caused by background subtraction errors, inadequate fitting ranges, confusion with exponential fall-offs at the largest events, small-number statistics, or may represent a non-SOC process altogether. The distinction between SOC processes and non-SOC processes is tabulated in the last column of Tables 1 and 2.
2. The means and standard deviations of the observed power law slopes agrees well with the theoretical predictions of the standard FD-SOC model (in 18 out of 23 astrophysical phenomena), with $\alpha_F = 1.80$ for the flux slopes and $\alpha_E = 1.67$ for the fluence slopes, after elimination of non-SOC systems.
3. Five outliers of astrophysical phenomena are identified and interpreted in terms of non-SOC systems, namely coherent radio bursts ($\alpha_F = 1.29 \pm 0.12$), solar energetic particle (SEP) events ($\alpha_F = 1.36 \pm 0.26$ and $\alpha_E = 1.34 \pm 0.15$), random radio bursts ($\alpha_F = 4.80 \pm 0.10$), and pulsar glitches ($\alpha_E = 1.90 \pm 0.78$), while all other cases are consistent with the standard FD-SOC model. Coherent radio bursts include type I and type III solar radio bursts and can be fitted with a nonlinear flux-volume relationship, as expected for coherent radiation mechanisms. Random radio bursts can be explained with the exponential fall-off sampled at the largest events of a size distribution according to Poisson statistics, which can assume any steep power law slope of $\alpha_F \gtrsim 3$. The flatter power law slope observed in SEP events indicates that not all flares produce protons, which appear to have a larger threshold in small solar flares. Pulsar glitches are clearly non-SOC processes that cannot be fitted by power law functions, given the observed large standard deviations ($\alpha_F = 1.90 \pm 0.78$). Hence, size distributions, their slopes α_x , and their outliers provide a valuable diagnostic of erroneous power law fits and non-SOC processes.

Future efforts on self-organized criticality models may focus on (i) improved precursor background subtraction errors (for instance when the flaring Sun eclipses the galactic center or other celestial X-ray sources), (ii) inadequate fitting ranges (which occur in the presence of strong deviations from ideal power law fits), (iii) combined fitting of power law functions and exponential fall-offs near the largest events, and (iv) small-number statistics (requiring larger data sets). Further tasks are the calculation of realistic fluences and energies, especially the estimates and frequency of the largest events that are essential when extrapolating the SOC statistics of extreme events. Other research subjects in SOC statistics are the extreme events of natural catastrophes, such as earthquakes, forest fires, wild fires, mountain slides, mud slides, hurricanes, taifuns, global climate changes, epidemics and pandemics (such as Covid-19), for which SOC models all have been found to be relevant.

ACKNOWLEDGMENTS

Acknowledgements: We acknowledge constructive and stimulating discussions (in alphabetical order) with Arnold Benz, Sandra Chapman, Paul Charbonneau, Henrik Jeldtoft Jensen, Adam Kowalski, Sam Krucker, Alexander Milovanov, Leonty Miroshnichenko, Jens Juul Rasmussen, Karel Schrijver, Vadim Uritsky, Loukas Vlahos, and Nick Watkins. This work was partially supported by NASA contract NNX11A099G “Self-organized criticality in solar physics” and NASA contract NNG04EA00C of the SDO/AIA instrument to LMSAL.

REFERENCES

- Aschwanden, M.J., Dennis, B.R., and Benz, A.O. 1998, *Logistic avalanche processes, elementary time structures, and frequency distributions of flares*, ApJ 497, 972.
- Aschwanden, M.J. 2011a, *Self-Organized Criticality in Astrophysics. The Statistics of Nonlinear Processes in the Universe*, Springer-Praxis: New York, 416p.
- Aschwanden, M.J. 2014, *A macroscopic description of self-organized systems and astrophysical applications*, ApJ 782, 54.
- Aschwanden, M.J. 2015, *Thresholded power law size distributions of instabilities in astrophysics*, ApJ 814.
- Aschwanden, M.J. 2013a, in *Theoretical Models of SOC Systems*, chapter 2 in *Self-Organized Criticality Systems* (ed. Aschwanden M.J.), Open Academic Press: Berlin, Warsaw, www.openacademicpress.de p.21.
- Aschwanden, M.J. 2013b, *Self-Organized Criticality Systems in Astrophysics (Chapter 13)*, in “Self-Organized Criticality Systems” (ed. Aschwanden, M.J.), Open Academic Press: Berlin, Warsaw, p.439.
- Aschwanden, M.J., Crosby, N., Dimitropoulou, M., Georgoulis, M.K., Hergarten, S., McAteer, J., Milovanov, A., Mineshige, S., Morales, L., Nishizuka, N., Pruessner, G., Sanchez, R., Sharma, S., Strugarek, A., and Uritsky, V. 2016, *25 Years of Self-Organized Criticality: Solar and Astrophysics*, Space Science Reviews 198, 47.
- Aschwanden, M.J. 2019a, *New millennium solar physics*, Springer Nature: Switzerland, Science Library 458.
- Aschwanden, M.J. 2021, *Finite system-size effects in self-organizing criticality systems*, ApJ 909.
- Aschwanden, M.J. 2022, *The fractality and size distributions of astrophysical self-organized criticality systems*, ApJ 934 33.
- Aschwanden, M.J. and Gogus, E. 2024, *Testing the universality of self-organized criticality in galactic, extra-galactic, and black-hole systems*, ApJ (in press).
- Aschwanden, M.J. 2025, *Power Laws in Astrophysics. Self-Organized Criticality Systems*, Cambridge University Press: Cambridge.
- Bak, P., Tang, C., and Wiesenfeld, K. 1987, *Self-organized criticality: An explanation of $1/f$ noise*, Physical Review Lett. 59(27), 381.
- Bak, P. 1996, *How Nature Works. The Science of Self-Organized Criticality*, Copernicus: New York.
- Benz, A.O. 1993, *Plasma Astrophysics*, Kluwer Academic Publishers: Dordrecht, The Netherlands.
- Boyd, T.J.M. and Sanderson, J.J. 2003, *The Physics of Plasmas*, Cambridge University Press: Cambridge.
- Cairns, I.H. 2004, Properties and interpretations of giant micropulses and giant pulses from pulsars, ApJ 610, 948-955.
- Charbonneau, P. 2017, *Natural complexity: A modeling handbook*, Princeton University Press, Princeton, New Jersey.
- Clinger, E., Reames, D., Kahler, S., and Cane, H. 1991, *Size distribution of solar energetic particle events*, Internat. Cosmic Ray Conf. 22nd, Dublin, LEAC A92-36806 15-93, NASA:Greenbelt, p.2:1.
- Clinger, E. and D’Huys, E. 2018, *Size distributions of solar proton events and their associated soft X-ray flares*, ApJ 864, 48/1, 11.
- Galam, S. 2012, *Sociophysics. A physicist’s modeling of psycho-political phenomena*, Berlin: Springer.
- Jensen, H.J. 1998, *Self-Organized Criticality. Emergent Complex Behavior in Physical and Biological Systems*, Cambridge University Press: Cambridge.
- Ilachinski, A. 2001, *Cellular automata*, World Scientific: New Jersey, 840p.
- Iwai, K., Masuda, S., Miyoshi, Y., Tsuchiya, F., Morioka, A., and Misawa, H. 2013, *Peak Flux Distributions of Solar Radio Type-I Bursts from Highly Resolved Spectral Observations*, ApJ 768, L2.
- Hergarten, S. 2002, *Self-Organized Criticality in Earth systems*, Springer: Berlin.
- Kahler, S.W. 2013, *Does a Scaling Law Exist between Solar Energetic Particle Events and Solar Flares?*, ApJ 769, 35.
- McAteer, R.T.J., Aschwanden, M.J., Dimitropoulou, M., Georgoulis, M.K., Pruessner, G., Morales, L., Ireland, J., and Abramenko, V. 2016, *25 Years of Self-Organized Criticality: Numerical Detection Methods*, SSRv 198, 217.
- Melatos, A., Peralta, C., and Wyithe, J.S.B. 2008, *Avalanche Dynamics of radio pulsar glitches*, ApJ 672, 1103-1118.

- Mercier, C. and Trottet, G. 1997, *Coronal radio bursts: A signature of nanoflares ?*, ApJ 484, L65.
- Ning, Z., Wu, H., and Meng, X. 2007, *Frequency distributions of microwave pulses for the 18 March 2003 solar flare*, Sol.Phys. 242, 101.
- Pruessner, G. 2012, *Self-Organised Criticality. Theory, Models and Characterisation*, Cambridge University Press: Cambridge.
- Scott, A.C. 2007, *The nonlinear universe: chaos, emergence, life*, Springer: Berlin, 364 p.
- Sharma, A.S., Aschwanden, M.J., Crosby, N.B., Klimas, A.J., Milovanov, A.V., Morales, L., Sanchez, R., and Uritsky, V. 2016, *25 Years of Self-Organized Criticality: Space and Laboratory Plasmas*, SSRv 198, 167.
- Sornette, D. 2004, *Critical phenomena in natural sciences: chaos, fractals, self-organization and disorder: concepts and tools*, Springer, Heidelberg, 528 p.
- Sturrock, P.A. 1994, *Plasma Physics*, Cambridge University Press: Cambridge
- Uritsky, V.M., Klimas, A.J., Vassiliadis, D., Chua, D., and George Parks 2002, *Scale-free statistics of spatiotemporal auroral emissions as depicted by POLAR UVI images: Dynamic magnetosphere is an avalanche system*, JGR 107, A12, 1426,
- Watkins, N.W., Pruessner, G., Chapman, S.C., Crosby, N.B., and Jensen, H.J. 25 Years of Self-organized Criticality: *Concepts and Controversies*, 2016, SSRv 198, 3.

Table 1. Astrophysical phenomena (column 1), number of flux data sets N_F (column 2), the power law slope of flux distributions α_F (column 3), the number of fluence data sets N_E (column 4), the power law slope of fluence or energy α_E (column 5), and the interpretation of SOC and non-SOC models (column 6).

Astrophysical phenomena	Power law slope		Power law slope		Theoretical Interpretation
	N_F	α_F	N_E	α_E	
Solar Flare Hard X-Rays (HXR)	20	1.74±0.11	9	1.56±0.11	SOC
Solar Flare Soft X-Rays (SXR)	10	1.87±0.10	5	1.79±0.35	SOC
Solar Nanoflares (EUV)	12	1.68±0.16	0	...	SOC
Solar Incoherent Radio Bursts	7	1.80±0.21	0	...	SOC
Solar Coronal Mass Ejections (CME)	5	2.01±0.35	6	1.84±0.41	SOC
Solar Wind (WIND)	3	...	13	1.70±0.17	SOC
Magnetospheric Auroras	12	1.79±0.21	10	1.60±0.13	SOC
Terrestrial Gamma-Ray Flashes (TGF)	0	...	3	1.73±0.40	SOC
Stellar Flares	15	1.82±0.37	0	...	SOC
Stellar Flares KEPLER	44	1.87±0.29	0	...	SOC
Stellar Flares (TESS)	5	2.27±0.19	0	...	SOC
Active Galactic Nuclei (AGN)	2	1.73±0.19	0	...	SOC
Black-Hole Systems (BH)	1	1.65±0.17	1	1.73±0.25	SOC
Blazars (BL)	2	1.98±0.08	2	1.63±0.17	SOC
Fast Radio Bursts (FRB)	0	...	13	1.67±0.12	SOC
Gamma Ray Bursts (GRB)	5	2.10±0.25	5	1.68±0.24	SOC
Soft Gamma Ray Repeaters (SGR)	2	1.88±0.06	18	1.68±0.12	SOC
X-Ray Binaries (XB)	6	1.52±0.45	4	1.53±0.04	SOC
Observations Means	15	1.85±0.19	12	1.67±0.09	SOC
FD-SOC Prediction		1.80		1.67	SOC

Table 2. Statistical outliers of astrophysical phenomena (see discussion in Section 2.6).

Astrophysical phenomena	Power law slope		Power law slope		Theoretical Interpretation
	N_F	α_F	N_E	α_E	
Solar Coherent Radio Bursts	5	(1.29±0.12)	0	...	gen-SOC, $\gamma \approx 2$
Solar Energetic Particles (SEP)	7	(1.36±0.26)	12	(1.34±0.15)	gen-SOC, $\gamma \approx 2$
Cosmic Rays	0		3	(3.02±0.03)	gen-SOC, $D_V = 1.0$
Solar Random Radio Bursts	4	(4.80±0.10)	0	...	non-SOC, random
Pulsar Glitches	3	(1.90±0.78)	0	...	non-SOC, erratic

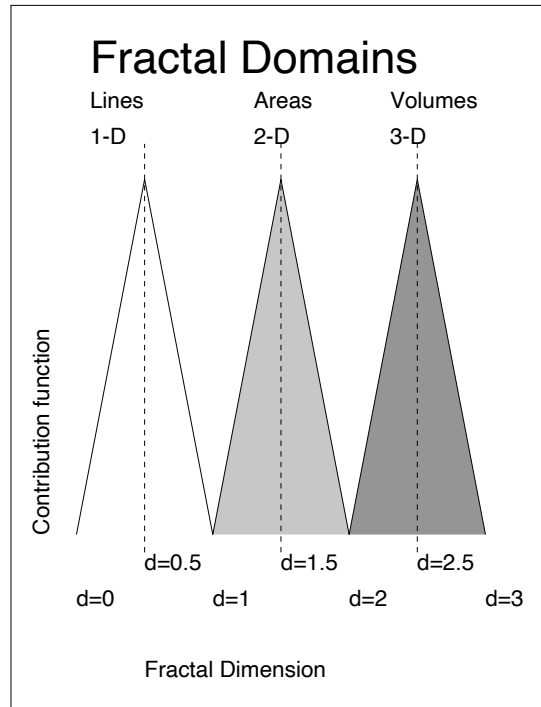


Figure 1. The contribution function to the three fractal domains (1-D lines, 2-D areas, and 3-D volumes) is illustrated as a function of the fractal dimension $0 \leq d \leq 3$. The mean fractal dimensions are $d=0.5$, 1.5 , and 2.5 in these 3 domains.

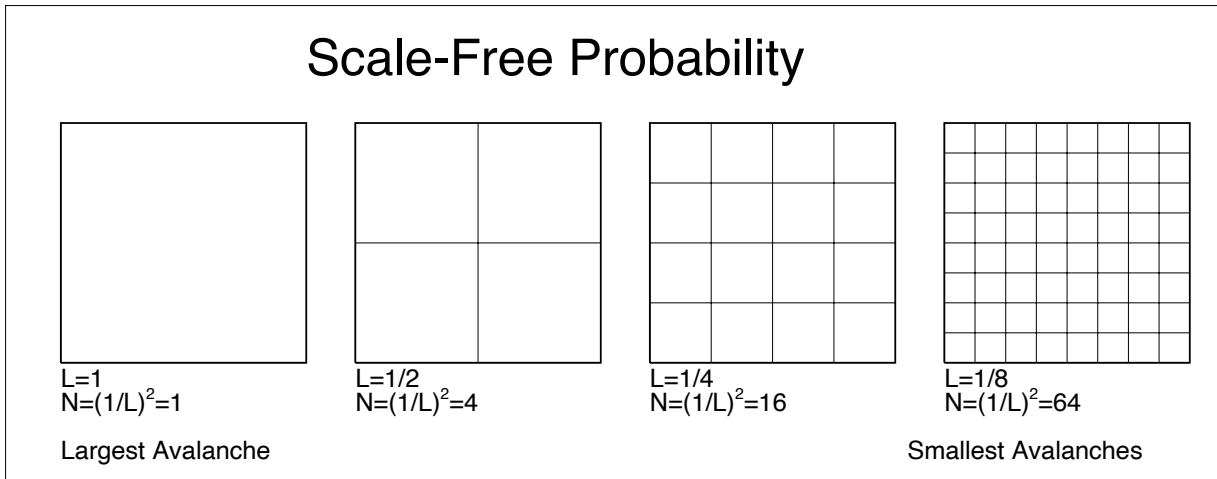


Figure 2. The scale-free probability is illustrated by segmenting the largest avalanche area (on the left side) into smaller avalanche areas (on the right side). While the length scale L decreases by a factor of 2 in each frame, the probability increases reciprocally by a factor of $N = 2^d = 4$ for the Euclidean dimension of $d = 2$, obeying the reciprocal scaling law $N = L^{-d}$.

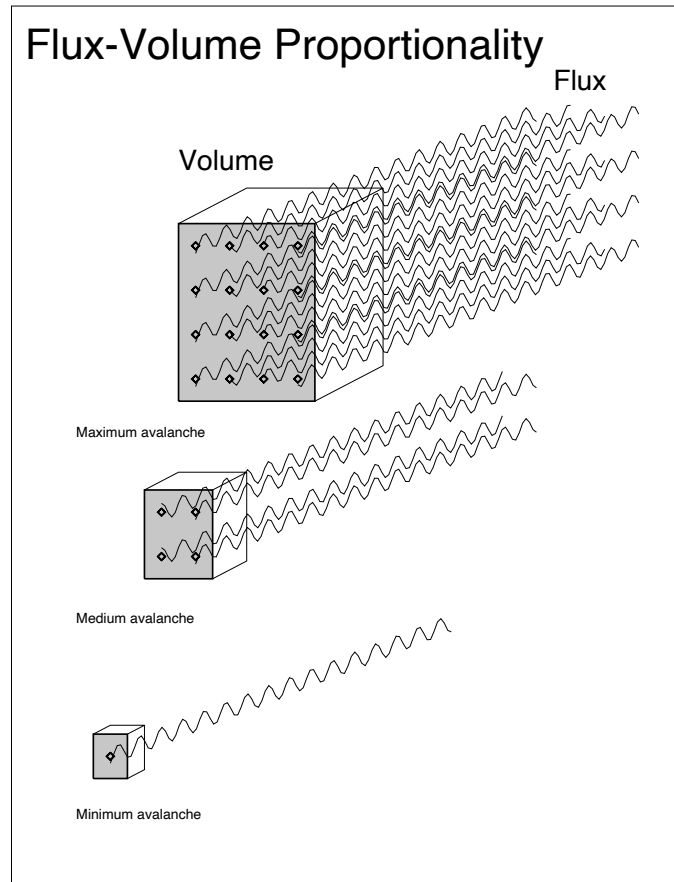


Figure 3. The relationship between the fractal volume V and the observed flux F is depicted for three different avalanche sizes, $F \propto V$.

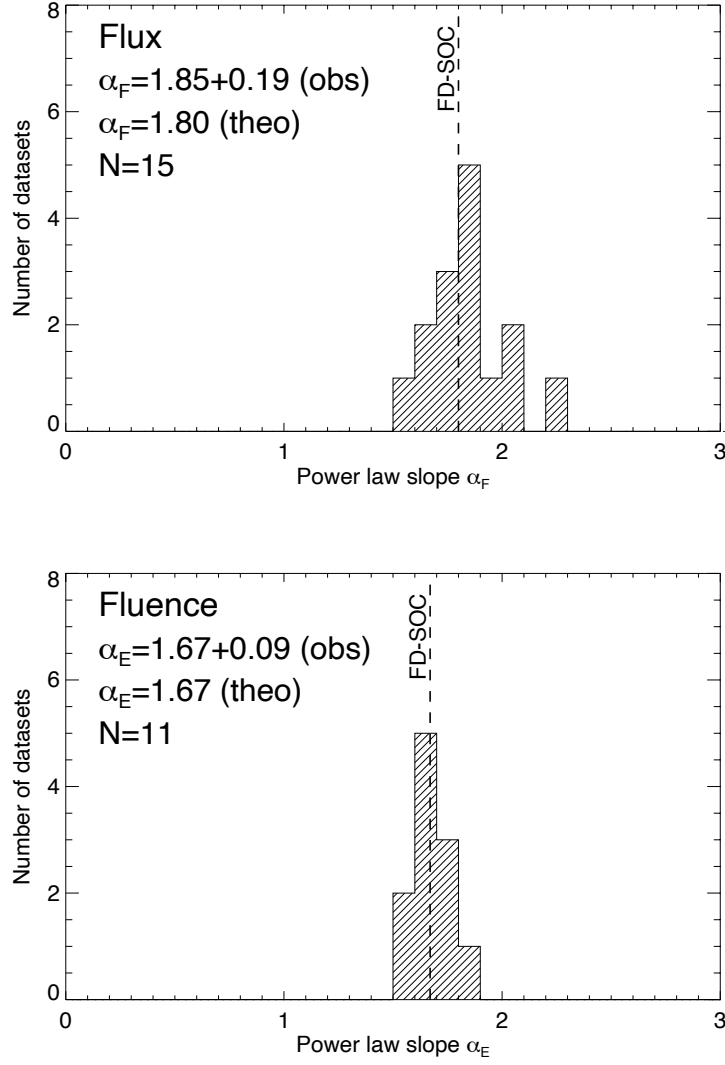


Figure 4. Histograms of power law slopes α_F for fluxes F (top panel) and of power law slopes α_E for fluences E (bottom panel), where each statistical element corresponds to a different astrophysical phenomenon, as tabulated in Table 1. The number of phenomena is indicated with the symbol N , and the theoretical FD-SOC prediction is indicated with a vertical dashed line.